KOM
CORROSION AND MATERIAL PROTECTION JOURNAL
ORIGINAL ARTICLE
sciendo

Comparative investigation on the influence of metakaolin, metaillite and steel slag as SCMs in mortar on the corrosion behavior of embedded steel

Achenbach, R., Raupach, M.
Institute of Building Materials Research (ibac), RWTH Aachen University
E-mail: achenbach@ibac.rwth-aachen.de

With the aim of saving CO_2 in cement production, various approaches are currently being pursued in the development of new materials. One possibility is to reduce the ratio of clinker to cement by using supplementary cementitious materials (SCMs). Some SCMs like fly ash or granulated blast furnace slag have been used successfully in cement for a long time and their use is covered by standards. Since the availability of these materials cannot be ensured in the long term, alternative additives are also being tested. The results presented here were obtained as part of a joint research project that was carried out in cooperation with the Bauhaus University Weimar. In this study, three different SCMs are investigated with regard to their effect on the corrosion of steel embedded in mortars: A metakaolin, a metaillite, and a modified steel mill slag were each tested at a proportion of 30 wt.% in a CEM I reference cement. In the two-stage tests, the passivation behavior of steel in mortars was first investigated in electrochemical tests. Based on this, tests were carried out in leached solutions of the different binders with different Cl^-/OH^- ratios.
The results show that all the blended types of cement investigated provide passivation of the steel in mortar. The use of the calcined clays metakaolin or metaillite resulted in higher polarization resistances and lower passive current densities as well as increased electrical resistivities, especially for metakaolin. The steel in mortar with the steel mill slag showed comparable electrochemical behavior to the OPC mortar. The tests in leached solutions slightly indicate a higher corrosion-inducing Cl^-/OH^- ratio when using metakaolin or steel mill slag.

INTRODUCTION

To provide durability of reinforced structures, the first step is the passivation of the embedded steel in the concrete. The pH of the concrete pore solutions of OPC and blended cements is between 12.5 and 13.8 [1] and provides a large amount of OH^- ions. An oxide layer of Fe_3O_4 is formed which further oxidizes to Fe_2O_3 on the electrolyte side [2–5]. The Fe_3O_4/ Fe_2O_3 layer is very dense and relatively constant in thickness and prevents anodic iron dissolution of the underlying steel [6]. On the electrolyte side, further oxidation processes may take place and form a less dense, layer with variable thickness consisting of $Fe(OH)_3$ and Fe_2O_3 [7]. When external polarization is applied, the formation of the passive film is depending on the electrode potential [7,8]. Without external polarization a less negative open circuit potential (OCP) is an indication for a lower probability of corrosion [9,10].

Many investigations have been carried out, to study the passivation behavior of steel rebars in concrete, mortar, and artificial pore solutions representing OPC. In comparative tests in mortar and artificial pore solution, the passivation process is faster in solution. This can be attributed mainly to the fact that the pH of the artificial solution is high from the beginning of the test and the pH in the fresh mortar rises over time since the mixing water is initially pH neutral [11,12].

The depassivation process is often initiated by chlorides when a critical content is exceeded at the steel surface. The threshold value depends on various factors: The composition of the pore solution and the properties of the steel surface, as well as the environmental conditions such as temperature, are relevant in the case of tests in solution and in mortar. The influence of the pore structure, reactions at the pore walls, and the moisture state of the material, on the other hand, are not considered in tests with artificial solutions [13,14].

The pH value is often cited as the most important parameter influencing the critical corrosion-inducing chloride content in the pore solution. Therefore, it is often expressed as a critical ratio of Cl^-/OH^- ions. For alkaline solutions representing the pore solution of OPC, studies are available on the critical corrosion initiating Cl^-/OH^- ratio. Hausmann [15] gives values between 0.66 and 1.4 in artificial pore solution and mentions that in con-crete with good quality and few air voids, values up to 3 are also possible. The critical ratio is also depending on the oxygen availability [13,15–17].

The current state of knowledge on the influence of the SCMs studied here on the passivation behavior of embedded steel and corrosion-inducing chloride content

varies: While some studies on concrete [18–21], mortar [22,23], and cement paste [24] are already available for the use of metakaolin as well as a review on durability by Homayoonmehr et al. [25], no such studies are known for the use of metaillite or steel slag.

Zhang et al. [18] investigated the corrosion rate of carbon steel in OPC concrete without and with different percentages of substitution by metakaolin. The specimens were exposed to a 3.5 % NaCl solution. They observed lower corrosion rates for a replacement of up to 15 wt. % of OPC by metakaolin but a higher corrosion rate, when 20 wt. % OPC was replaced by metakaolin. Batis et al. [23] also stated a beneficial effect of metakaolin for corrosion protection up to a replacement of 15 wt. %, but not for 20 wt. %. Ghanem et al. [24] replaced 5 to 20 wt. % of OPC with metakaolin in paste samples and exposed them to 3.5 % NaCl. The samples with 20 wt. % metakaolin show the lowest corrosion rate estimated by Tafel plots after 90 days of exposure. Also, the 10 wt. % sample shows lower corrosion rates than the OPC reference but the 5 and 15 wt. % metakaolin samples show higher corrosion rates than the OPC samples. Borade and Kondraivendhan [26] investigated the corrosion behavior in the macrocell test setup according to ASTM G109 with substitution with metakaolin of 15 % at different w/b values. They, as well, observed lower macrocell corrosion currents when metakaolin was used and applied wetting/drying cycles with NaCl solutions of varying chloride content, which typically result in higher chloride content in the concrete than exposure to NaCl solution without drying periods [27]. However, in all these tests it should be considered that the use of metakaolin refines the microstructure [19,28] and the chloride migration coefficient is considerably lower, so that the same chloride concentration is not present at the steel surface as in the test specimens used for comparison. Güneyisi et al. [20] investigated concretes with 0 %, 5 %, and 15 % metakaolin replacement levels in concrete specimens with admixed chlorides. They also observed lower corrosion rates in the metakaolin samples, which could not be attributed to a lower chloride concentration on the steel surface, but rather to the increased electrolyte resistance of metakaolin blended concretes compared to OPC. Although comparison of corrosion rates is problematic when the anodic area is unknown, there seems to be agreement in principle that the use of metakaolin has a positive effect on the corrosion protection of the reinforcement, but it is not yet completely clear up to which substitution rate. There are no known studies on the influence of metakaolin on corrosion behavior at a substitution rate of more than 20 wt. %.

For the influence of steel slag, as secondary raw material from the processing of pig iron into steel in the steel mill, on the corrosion behavior of embedded steel, no investigations are known. The study of the influence of metaillite on the durability of steel reinforcement has also received little attention so far.

Therefore, the investigations carried out here aimed to compare the three different SCMs, each with a substitution rate of 30 wt. % in CEM I, and thus to obtain initial findings for the influence of steel mill slag and metaillite on the corrosion behavior and to extend the state of knowledge regarding metakaolin by a higher substitution rate. Both, the influence of the SCMs on the passivation behavior was investigated in mortar, and first tentative tests on the critical corrosion-inducing Cl^-/OH^- ratio were carried out in leached solutions.

In both cases, the same electrochemical test methods were used, and the results were evaluated with respect to the reference tests without SCMs.

EXPERIMENTAL

The experimental investigations are separated into two parts: In part I the passivation behavior of steel embedded in mortar specimens made with three different alternative SCMs was investigated. In part II investigations in leached solutions of the same binder types have been carried out with three different Cl^-/OH^- ratios each. An OPC was used as reference series in both parts.

Tab. 1. Chemical composition of the binders, values in wt. %

	SiO_2	Al_2O_3	Fe_2O_3	CaO	MgO	MnO	TiO_2	K_2O	Na_2O	SO_3	LOI
Ref 1	20.50	4.70	2.90	63.20	1.30	0.03	0.20	1.22	0.28	3.20	2.40
CC I 70 wt.% Ref 1 + 30 wt.% Metaillite	29.62	5.85	2.56	36.12	1.09	0.02	0.31	1.18	0.22	2.26	20.18
CC II 70 wt.% Ref 1 + 30 wt.% Metakaolin	30.30	16.30	2.20	44.30	1.10	0.00	0.60	0.90	0.20	2.40	1.70
LD 70 wt.% Ref 1 + 30 wt.% BOF slag	17.69	2.98	7.24	47.69	1.21	0.60	0.31	0.59	0.14	1.95	19.20

Tab. 1 shows the chemical composition of the different binders investigated and the identifiers used for the different test series.

The binder types consisted of 70 wt. % of the reference OPC a CEM I 42.5 R and 30 wt. % of the different SCMs. In series CC I a calcined illite-based clay was used. In CC II a commercially available metakaolin was added and in series LD a modified steel slag from a BOF process was used. A detailed description of the materials and the characterization of their hydration behavior can be found in [28].

Passivation in mortar without Chlorides

Mortars were made from the binders described above. For this purpose, CEN Standard sand according to EN 196-1 [29] (0.08 – 2.0 mm grain size) was mixed with the binder in a ratio of 3:1. The w/b ratio was 0.5. To achieve sufficient workability, a commercially available superplasticizer based on naphthalene sulfonate was used in the CC I (0.8 wt.-%) and CC II series (2.2 wt. %).

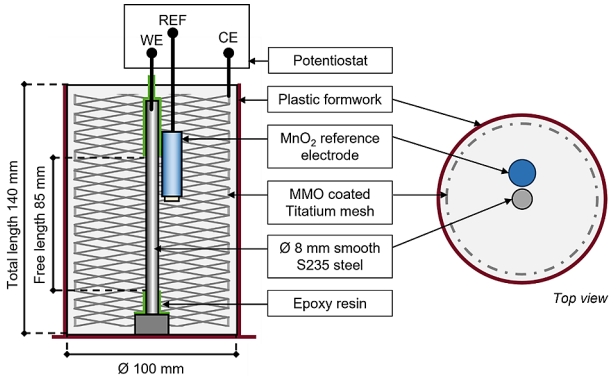


Fig. 1. Schematic representation of the specimen design

For the four different types of binder, three specimens each were produced. Fig. 1 shows a schematic illustration of the specimen in the three-electrode design.

The cylindrical mortar specimens contain the working electrode made of steel in the center, an embedded MnO_2 reference electrode, and a counter electrode made of MMO-coated titanium mesh. The MnO_2 reference electrodes have a potential of 434 mV vs. SHE. The counter electrode was arranged in a cylindrical form around the working and reference electrode a few millimeters inside the outer specimen surface. The working electrodes made of S235 smooth black steel were sandblasted. The elemental composition determined by OES is given in Tab. 2.

After casting the specimens were covered with plastic sheets, kept in laboratory climate (20 °C, 50 % r. h.), and connected to the potentiostat. At the age of seven days, the plastic sheets were removed. The specimens stayed in the formwork for the whole measurement.

Electrochemical tests in mortar

The electrochemical tests were performed with potentiostats from Gamry Instruments. Up to the age of 28 days, the open circuit potential (OCP) was measured vs. the embedded reference electrode and impedance spectra were taken daily. Because of the low polarization, these tests are considered to not influence the formation of the passive layer. On day 28 an anodic polarization curve starting at OCP was carried out. The measurement parameters are listed in Tab. 3.

After the measurements were completed, the test specimens were split, the working electrodes removed, visually inspected, and photographed. The epoxy sealings of the steel ends were removed to check the underlying steel surface for crevice corrosion.

Tab. 2. Elemental composition of the steel, values in %

Fe	Mn	Cu	Si	Ni	C	Cr	Sb	Mo	S	Sn	As	Te	P
98.0	0.71	0.39	0.212	0.160	0.114	0.092	0.048	0.031	0.030	0.029	0.025	0.024	0.020

Tab. 3. Measurement scheme for each mortar specimen

Method	Measurement parameters	Measuring interval
Potential measurements	Reference electrode: MnO_2 Sample period: 1 sec; Stability criterion: ± 0.1 mV in 10 sec	Daily from day 0 to 28
EIS	Frequency range: 0.001 Hz to 10 kHz; Voltage: ±10 mV_{rms} around OCP; 5 points per decade	Daily from day 1 to 28
Anodic polarization curve	Voltage: 0 to 2000 mV starting from OCP; Feed rate: 2 mV/min; Sample period: 120 sec	Once at the end (day 28)

Corrosion in leached solutions without and with chlorides

To investigate the corrosion behavior under the influence of chlorides, leached solutions with different Cl^-/OH^- ratios were prepared. Therefore, cement pastes were made by mixing one part of the binders listed in Tab. 1 with two parts of deionized water. The pastes were prepared in bottles which were shaken in an overhead shaker at 20 rpm for 24 hours. The test solutions were filtered by means of a vacuum pump. The solutions from different bottles of the same series were homogenized with each other and provided the test solution without chlorides ($Cl^-/OH^- = 0$). Portions of these solutions were separated and mixed with chlorides: The pH and temperature were measured, the OH^- content was calculated and NaCl was added to achieve a Cl^-/OH^- ratio of 1 respectively 3. The used NaCl concentrations are also given in Table 4.

The measurement cells in the three-electrode setup were operated inside a glove box which was filled with 20.5 % O_2 in N_2 to prevent carbonation of the testing solutions. The glove box was placed in laboratory climate (20 °C, 50 % r. h.) The same S235 smooth black steel, also sandblasted, was used as described for the mortar tests. As counter electrodes also MMO-coated titanium meshes in a cylindrical arrangement around working and reference electrodes were used. The reference electrodes were Hg/HgO electrodes filled with 1 M NaOH. Their potential is 140 mV vs SHE.

Electrochemical tests in leached solutions

One experiment per series and Cl^-/OH^- ratio was carried out. The working electrodes were preconditioned by cathodic polarization of –1000 mV vs. SHE for 10 minutes to remove any oxide layers by hydrogen evolution that might be present. The preconditioning was done in a separate measurement cell filled with deionized water to keep the testing solutions unaltered. Then the working electrodes were installed in the measurement cells with the leached solutions without chloride to let the steel passivate for four days. The duration until the potential values no longer change significantly was determined to be four days in the mortar tests, so this period was also provided for the passivation of the working electrodes in the solutions without chloride. On day five the working electrodes were set to another cell with the same solution but with a Cl^-/OH^- ratio of 0, 1, or 3. The measurement cells containing the solutions with chloride were also kept inside the glove box during the passivation time, to set them to the same conditions (temperature and glovebox atmosphere).

OCP was measured every hour during the testing period of seven days in total. Every day one EIS was done until day 7. The same measurement parameters as listed in Tab. 3 were applied.

RESULTS

All potential measurements are converted to the standard hydrogen reference for better comparability. Since the mean values from three test specimens are shown for the tests in mortar, the scatter is shown as the range between the minimum and maximum measured values. No scatter is given for the tests in solution since they are individual tests.

Passivation in mortar without Chlorides

The results of the investigations of the mortar specimens are presented in the following.

Potential measurements in mortar

Fig. 2 shows the results of the OCP measurements over 28 days. The readings of the different series are close to each other and the potential increases significantly in the first four days and steadily slightly thereafter. After 28 days, the measured values are between 50 and 100 mV. The measured values show a characteristic trend for the passivation process of the steel.

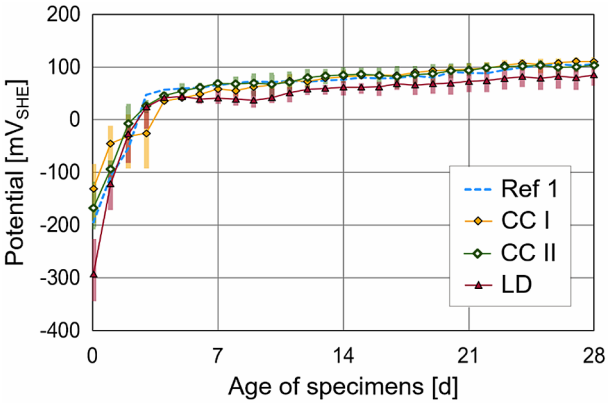


Fig. 2. Results from the OCP measurements in mortar, shown as mean value from three specimens; Scatter displayed as range between minimum and maximum value

EIS measurements and fit results in mortar

Fig. 3 shows an example of EIS measurements taken at different specimen ages during the passivation process of the working electrode in specimen 1, binder CC II.

The different frequency ranges allow the investigation of different electrochemical parameters [30,31]: The high-frequency region may be influenced by the capacitive behavior of the mortar, which leads to phase angles below zero. In the frequency region where the phase angle is zero (Bode), respectively the imaginary part Z_{imag} is zero (Nyquist), a purely ohmic resistance is measured, which represents the R_u as the electrical resistance of the mortar between the reference and

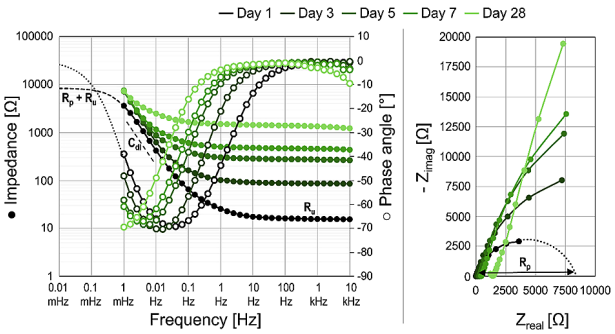


Fig. 3. Example of representative EIS results from CC II series; left: Bode plot, right: Nyquist plot

working electrode. It is easy to see, that the R_u increases over time. The frequency region where the phase angles are negative again (< 100 Hz) is influenced by the processes at the steel mortar interface. A low phase angle in this region indicates protective oxides on the steel surface [32]. The slope of the impedance curve in the small frequency region is dependent on the double-layer capacitance C_{dl}. A greater slope corresponds to a lower C_{dl}. In very low frequencies the polarization resistance R_p would cause the impedance to enter a plateau again, but this often cannot be seen in the measurement data because the measured frequency cannot be low enough: The system would not be stable during the long time needed for the measurement with very low frequencies. In the Nyquist plot, R_p would be reflected by the diameter of the semi-circle, which is analogously incomplete here. Within certain limits and under the assumption that the curve of the phase angle follows a symmetrical course, R_p can be determined through extrapolation, respectively fitting of an equivalent circuit. However, it can be seen from the curves shown here in the Bode and the Nyquist plot that a specification of R_p at a higher sample age becomes more and more speculative and approaches arbitrariness at day 28. R_p is mainly driven by charge transfer resistance but may also contain resistive components from diffusive processes [33].

The EIS data of each specimen was fitted using the Randles equivalent circuit with a CPE, shown in Fig. 4. Although there is an indication of a second time-constant in the high-frequency range in Fig. 3 at the older specimen

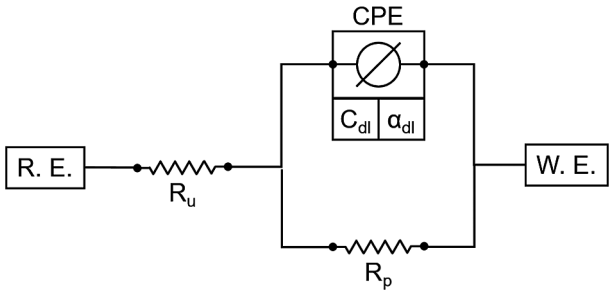


Fig. 4. Equivalent electrical circuit used to fit EIS data

age, which could be due to the capacitive influence of the mortar, all series were fitted with the equivalent circuit shown in Fig. 4. The high-frequency range (> 1 kHz) was excluded for the fit in order to investigate only the processes at the steel mortar interface.

The fit results of the EIS data from the mortar specimens are shown in Fig. 5 to 8. The ohmic resistance R_u (Fig. 5) depends on the electrical resistance of the mortar between the reference and working electrodes and thus on the specimen geometry. A conversion to a specific electrolyte resistance, which would be comparable with other measurements, is therefore not easily possible. However, since the specimen geometry is the same for all mortar test specimens, which is also supported by the low scatter of the R_u values from the same series, R_u can be used here to compare the electrolyte resistances with each other: The electrolyte resistances of the LD series is comparable to the reference series Ref 1. The mortars with the calcined clays CC I and CC II show higher electrolyte resistances, whereas the R_u of CC II is about ten times higher than for Ref 1 at the age of 28 days. The increase of the R_u values is a result of hydration and maybe also of drying.

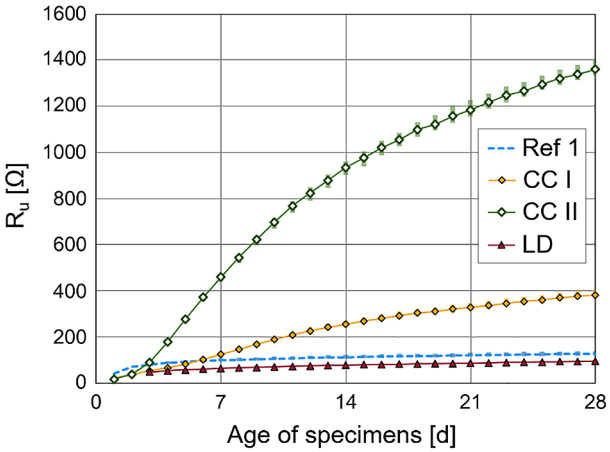


Fig. 5. Fit results from EIS measurements in mortar for R_u

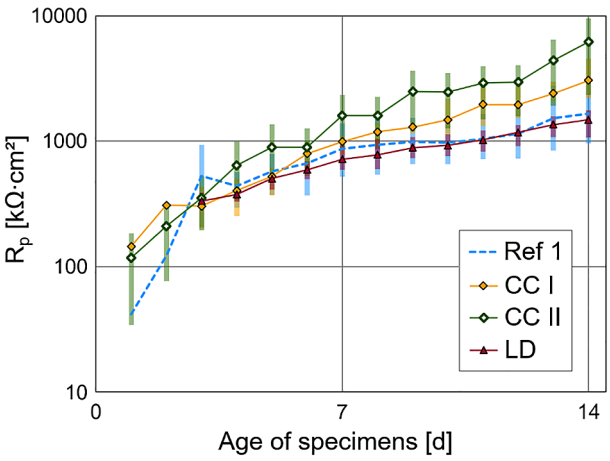


Fig. 6. Fit results from EIS measurements in mortar for R_p

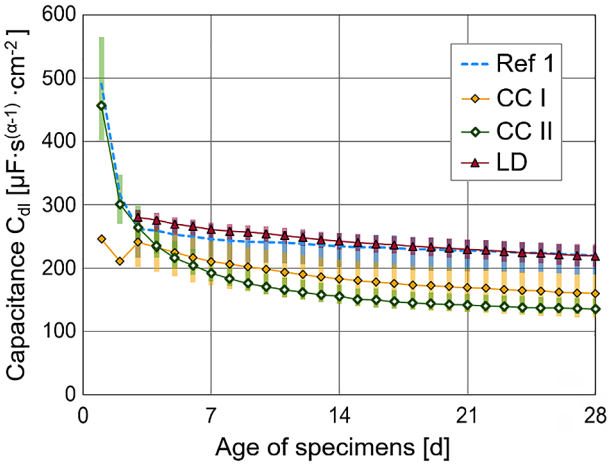


Fig. 7. Fit results from EIS measurements in mortar for C_{dl}

The polarization resistance R_p (Fig. 6) is subject to greater scatter and can only be reliably determined for the first 14 days of the measurement period. After that, R_p becomes too large to be determined in the smallest measured frequency range during the measurement. Despite this, a continuous increase in all polarization resistances can be seen and a higher polarization resistance for the CC I and CC II series than for LD and Ref 1.

The capacitance C_{dl} (Fig. 7) decreases during the passivation of the steel. Sánchez et. al [34] explain the decrease in capacitance by a reduced conductivity of Fe_2O_3 compared to Fe_3O_4: The steel side Fe_3O_4 layer forms first and then remains relatively constant in its thickness, while towards the electrolyte side, it further oxidizes to Fe_2O_3. The thickness of the layer on the electrolyte side then continuously increases over time, which is reflected in the reduction of the capacitance.

The values are overall rather high, as often observed in the literature [7,35–37], which could be an effect of the sandblasted steel surfaces. The capacitances evolve inversely proportional to the above described OCP values so that the values of the different measurements support each other and show the progress of passivation.

The factor α_{dl} takes the non-ideal behavior of the double layer as a capacitor into account, which also contains ohmic resistance components [31]. The fitted values for α_{dl} of all test specimens are in the range between 0.76 and 0.86, which supports the assumption of capacitive behavior.

Polarization curves in mortar

At the end of the measurements at the age of 28 days, an anodic polarization curve of every specimen was determined. These are displayed in Fig. 8. The displayed data is IR compensated based on the R_u determined by the EIS fit. All specimens show passive behavior, as no breakthrough potential occurs up to a voltage of around 850 mV_{SHE} where oxygen evolution leads to an increase in the current density. This behavior is consistent with the description of passive steel in mortar in [38]. The passive current densities of the CC series are slightly lower than for Ref 1 and LD.

The binder types with the higher polarization resistances and lower fit results for C_{dl} (CC I and CC II) show lower current densities.

The surfaces of the working electrodes removed after the end of the test show no signs of corrosion (see Fig. 9), which confirms the classification as passive systems. No crevice corrosion occurred under the coatings. Since the binder series with the lower capacitances and higher polarization resistances also show lower passive current densities, the current density curves show no fluctuations and the steel surfaces are free of signs of corrosion after the end of the test, it is assumed that the chosen measurement parameters were suitable.

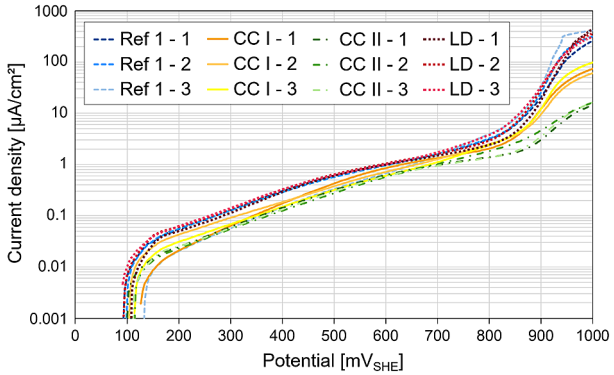


Fig. 8. Anodic polarization curves of all mortar specimens at the age of 28 days

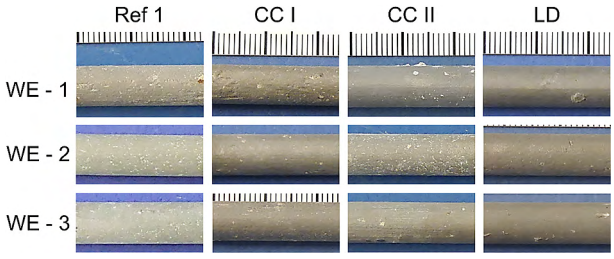


Fig. 9. Removed working electrodes after the tests in mortar

Corrosion in leached solutions with Chlorides

The results of the electrochemical measurements in the leached solutions without and with chloride are described in the following.

Verification of the test setup

A few questions were raised during the development of the experimental setup, which will be answered in the following on the basis of the measured values. On the one hand, it was important for the reliability of the experiments that the pH values of the leached solutions

Tab. 4. pH of leached solutions during the tests and NaCl concentrations calculated to set Cl^-/OH^-

	pH Start	pH Day 4	pH End/Day 7	NaCl concentration Cl^-/OH^- = 1	NaCl concentration Cl^-/OH^- = 3
	[–]			[g/l]	
Ref 1	13.7	13.6	13.6	26.1	78.3
CC I	13.6	13.6	13.6	23.3	69.8
CC II	13.6	13.6	13.6	23.8	71.4
LD	13.5	13.5	13.5	16.8	50.6

correspond to the realistic values of pore solutions. On the other hand, it was to be verified that the pH of the solutions was stable over time, and whether conducting the experiments in the glovebox with the mixture of O_2 and N_2 successfully prevented the carbonation of the solutions. For this purpose, the pH values of the experimental solutions were measured at different times. Tab. 4 lists the pH values measured by a glass electrode in the test solutions without chlorides at the beginning of the experiments, on day 4 and at the end of the experiments (day 7) and also the used NaCl concentration to reach the different Cl^-/OH^- ratios.

The pH of the leaching solutions is around 13.6 for the series Ref 1, CC I and CC II. The pH of the LD series is slightly lower at around 13.5. These are reasonable values that correspond to concrete pore solutions. The table also shows that the values remain stable over the test duration.

Another question concerning the experimental setup was whether moving the working electrodes to another measuring cell and the resulting short contact with air would influence the measured values. Therefore, the measuring cell was also changed after four days in the experiments without chloride (Cl^-/OH^- = 0).

Fig. 10 shows the results of the OCP measurements. After four days the working electrodes were set to another measuring cell. It can be seen that the potential values in the new cells are in good agreement with the values in the first cells and the change does not affect the measurement values in a great manner.

The OCP measurements also show, that the passivation process indicated by the increasing potentials is faster than in the mortar specimens, but the potentials stay at a slightly lower value of around 25 mV_{SHE} compared to the measurements in mortar. The values remain relatively stable from two days on, with just a very slight increase over time. Also, there is almost no difference between the different series.

Potential measurements in leached solutions with chloride

The results of the OCP measurements, were the working electrodes where set to measuring cells containing chloride are shown in Fig. 11 and 12.

When set to the solution with a Cl^-/OH^- ratio of 1 (see Fig. 11), the potential of the Ref 1 series shows a slight increase and then drops around 200 mV, whereas the potential of CC I decreases about 600 mV to a value of around –600 mV_{SHE}. Series LD shows a slight drop but recovers within half a day and the OCP values of series CC II seem not to be affected by the chloride.

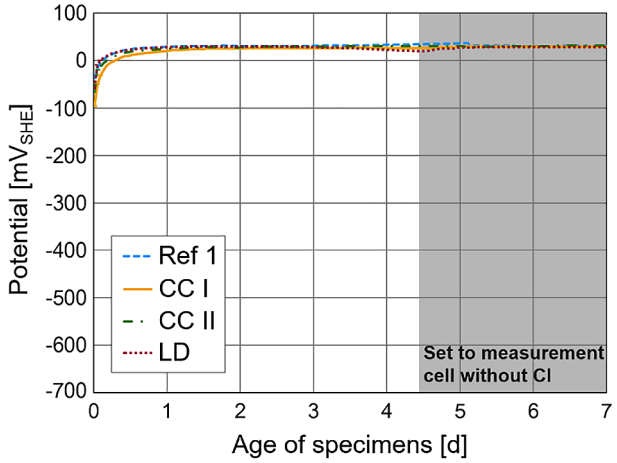


Fig. 10. OCP in solution without chloride with change of measurement cell

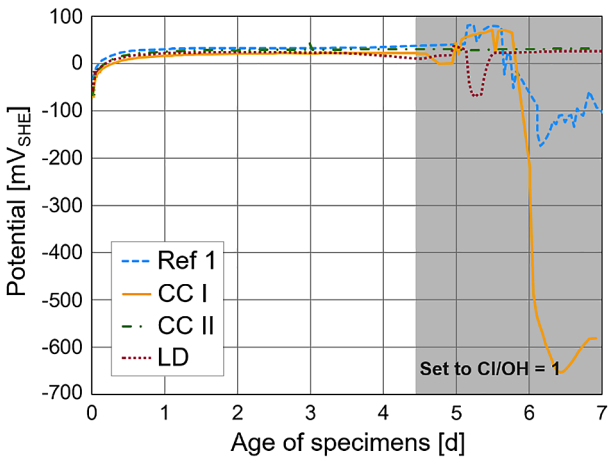


Fig. 11. OCP in solution, changed to measurement cell with Cl^-/OH^- = 1

When set to the solution with a Cl^-/OH^- ratio of 3 (see Fig. 12), the measured potential of all series drops immediately. The measured values of series Ref 1, CC I, and LD stabilize around –200 mV_{SHE} whereas CC I again shows the lowest potential at around –600 mV_{SHE}.

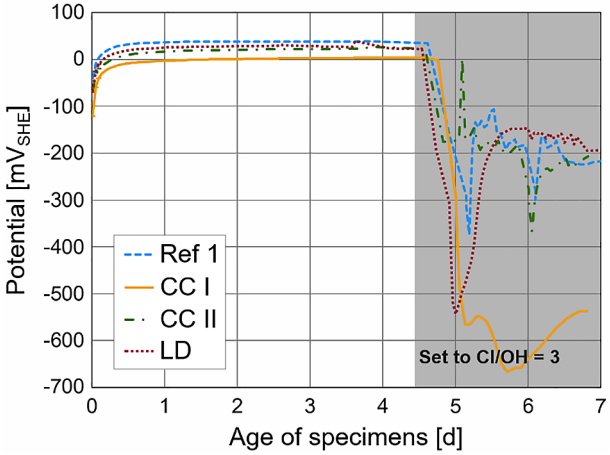


Fig. 12. OCP in solution, changed to measurement cell with Cl^-/OH^- = 3

EIS fit results of the tests in leached solutions without and with chloride

The EIS data from the investigations in solution were fitted with the same equivalent circuit as the mortar specimens, shown in Fig. 4. Analysis using a Kramers-Kronig fit [39,40] showed that not all the systems investigated were stable down to the smallest measured frequency of 1 mHz, so that the frequency range below 1 Hz was excluded before the fit. Thus, it was not possible to determine the polarization resistances for every EIS measurement. Polarization resistances could be determined at days 4 and 7, but not for series CC I. The fit results for R_u (exemplary), C_{dl}, and R_p where possible are shown below.

Fig. 13 shows the fit results for R_u exemplary for the measurements, where the working electrodes were set to the high chloride content. The results show, that R_u is very low compared to the mortar specimens and does not change over the first days, which was expected because there's no pore system and no hydration process and the solution is highly conductive. This conductivity even increases when chloride is added which results in a drop of R_u. After chloride addition, the LD series shows slightly higher R_u values than the other series, which is due to the fact that the LD series solution had a lower pH and therefore less chloride had to be added to adjust the same Cl^-/OH^- ratio.

Fig. 14 shows the fit results for C_{dl} when set to the solutions without chloride. The values are in the same order of magnitude as in the mortar tests but in a different order of the series. The values also develop inversely proportional to the potential measurement values, which also change only very slightly between days one and seven. In addition, it is confirmed here that moving the working electrodes to other measuring cells with the same solution does not affect the measured values.

Fig. 15 shows the fit results for C_{dl} when set to the solutions with chloride. To show the drastic increase of the capacitances in series CC I, it was necessary to choose the logarithmic scale. The observations of the OCP measurements can be confirmed here: The lower chloride content (Cl^-/OH^- = 1) hardly influences the measured values for the CC II and LD series and leads to a slight increase in capacitance for Ref 1. For series CC I, C_{dl} increases by several orders of magnitude. At the higher chloride content (Cl^-/OH^- = 3), all capacitances increase, but again only those of series CC I drastically.

The fit results for the corresponding α_{dl} of the experiments in solution are between 0.85 and 0.90for all tests, apart from series CC I: In tests with chloride the α_{dl} drop at day 6 and 7 to values between 0.5 and 0.7. Here, corrosion products may influence the steel surface.

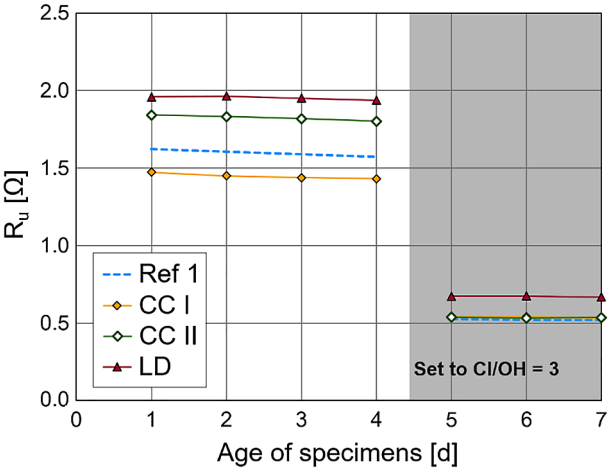


Fig. 13. Fit results from EIS measurements in solution for R_u; Set to measurement cells with Cl^-/OH^- = 3

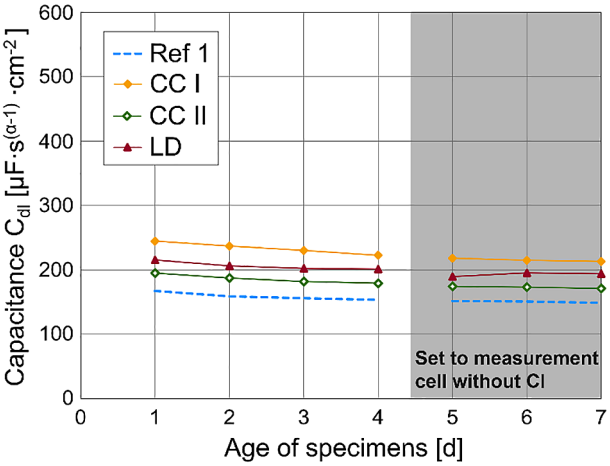
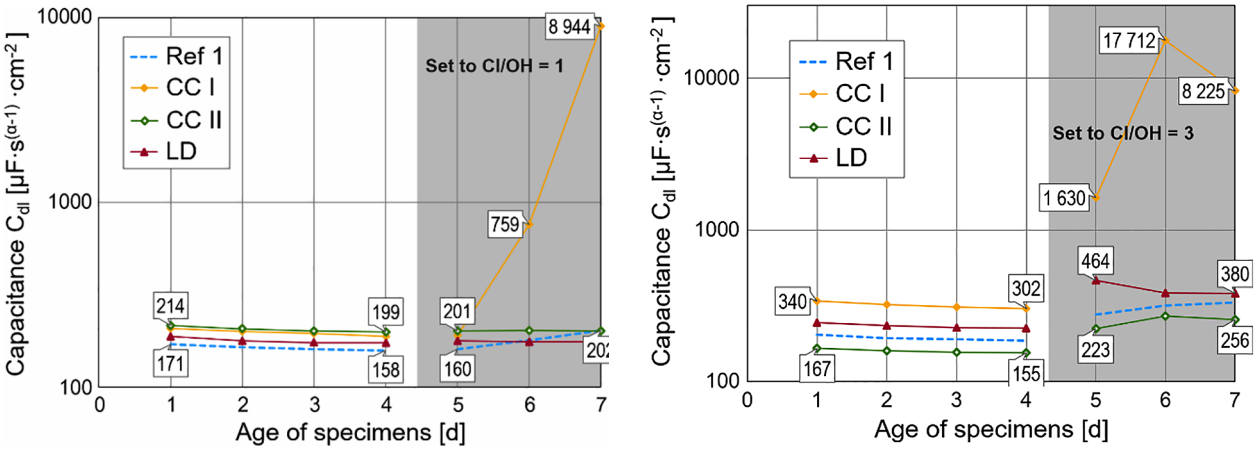


Fig. 14. Fit results from EIS measurements in solution for C_{dl}; Set to measurement cells without chloride



a) Cl^-/OH^- = 1 b) Cl^-/OH^- = 3

Fig. 15. Fit results from EIS measurements in solution for C_{dl}: set to measurement cells with chloride – a) Cl^-/OH^- = 1, b) Cl^-/OH^- = 3

Fig. 16 shows the fit results for the polarization resistances at days 4 and 7. The values for day 4 are the mean values of three tests. The scatter is shown as range between minimum and maximum value. No scatter is shown for the different chloride contents as this are single tests. The polarization resistances at day 7 when set to the measurement cell without chlorides are in the same magnitude as at day 4. When set to solutions containing chlorides the polarization resistances drop as expected: At Cl^-/OH^- = 1 the series Ref 1 showed the lowest polarization resistance what is analogous to the lower measured potential and the higher capacitances. The polarization resistances of series CC II and LD are just slightly lower than before the change to chloride solution what is also in good agreement with the potential measurements and the unchanged C_{dl} values. At Cl^-/OH^- = 3 series Ref 1, CC II and LD show lower polarization resistances what corresponds to the decrease in potential measurements. The R_p values for series CC I could not be determined.

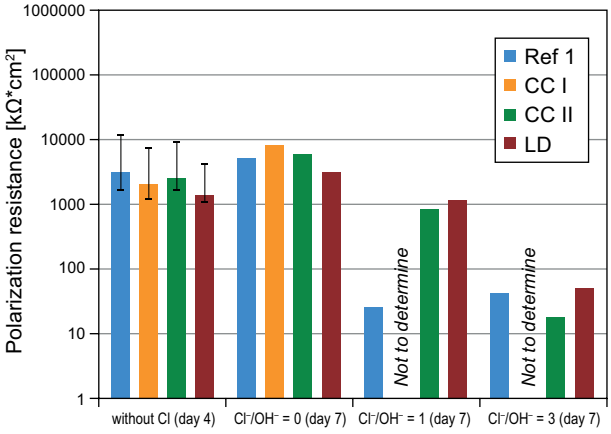


Fig. 16. Fit results from EIS measurements in solution for R_p; set to cells with different chloride contents

DISCUSSION

Comparability of investigations in mortar and leached solutions

The comparability of the tests in mortar and solution can be assessed because the same binders were used to produce the mortar specimens and the leached solutions. Also, the working electrodes in mortar and solution tests were from the same batch of steel and prepared the same way, apart from the fact that the working electrodes in the solution tests got a preconditioning with cathodic polarization, which would not have been possible in mortar tests without altering the mortar. The comparison of measured values in mortar and solution is discussed based on the tests without chlorides, as no tests in mortar with chlorides have been done yet. The measured OCP values are slightly lower in solution compared to mortar, which is in good agreement with [41]. The fit results of the capacitances also show good agreement measured in mortar and solution, apart from the R_u, which is, as expected, very low in solution and does not change over time. The relationship of the measured values of the individual series to each other will not be discussed here, since no scatter can be given for the tests in solution due to the small number of tests. In addition, Duffó et al. [41] recommend using artificial pore solutions with different chloride contents for comparing the corrosion behavior of different materials but do not consider extrapolation to mortar to be appropriate.

Reference series (Ref 1)

The reference series Ref 1 shows the expected results for a passive system in all mortar tests and the results of the different electrochemical measurements support each other. The only deviation results in comparatively high capacitances and passive current densities with regard to the steel surface. The capacitances are about the same

magnitude in mortar and solution. A consideration of the larger surface area of the sandblasted working electrodes compared to polished steel surfaces would lead to more comparable values to the literature. The same applies to all the test series here.

The corrosion-inducing Cl^-/OH^- ratio of Ref 1 seems to be around 1, as the potential values and polarization resistance drops, indicating a depassivation.

Metaillite (CC I)

The series CC I shows passivating behavior in the mortar tests. The electrolyte resistance is higher than in Ref 1 but lower than for the CC II series. The capacitances and current densities under polarization are lower and polarization resistances higher than for the Ref 1 series which indicated more protective passivation.

The observed behavior in the solution tests with chloride addition shows a corrosion-initiating Cl^-/OH^- ratio of below 1 with a large potential drop of –600 mV and comparatively high capacitances in the EIS measurements. This deviating behavior could be due to the chemical composition of the solution and is subject of further research.

Metakaolin (CC II)

The series CC II also shows passivating influence on the steel, with higher polarization resistances and lower capacitances and current densities indicating more protective passivation than the reference series. In addition, the electrolyte resistance of the mortar is around 10 times higher in comparison to the reference.

The corrosion-inducing Cl^-/OH^- in the leached solution seems to be between 1 and 3 and therefore also higher than that of the reference series.

BOF slag (LD)

The LD series shows passivating influence in the mortar tests with measurement values that are in good agreement with the reference series. Therefore, neither a negative nor a positive influence on the passivation behavior can be stated. No indication of corrosion-promoting substances could be detected.

The corrosion-inducing Cl^-/OH^- in the leached solution seems to be between 1 and 3 and therefore also higher than that of the reference series. It is to note that the pH of the leached solution of the LD series was slightly lower than for the other binder types. Therefore, the total chloride content at the same Cl^-/OH^- ratio was lower for this testing solution.

CONCLUSIONS & OUTLOOK

- All binders tested, allow for passivation of the steel.
- The addition of metakaolin significantly increases the electrolyte resistance of the mortar.
- No negative influence on passivation due to the addition of BOF slag (LD) could be detected.
- The addition of the calcined clays metakaolin or metaillite leads to higher polarization resistances and lower double-layer capacitances than OPC and also to lower current densities under polarization. Whether this leads to a better protection against chlorides must be investigated in further tests with a larger amount of samples.
- There was an indication for higher corrosion-initiating Cl^-/OH^- ratio due to the addition of metakaolin (CC II) or BOF slag (LD) but this statement is based on a small number of tests.

Acknowledgment

This research was funded by the German Research Foundation (DFG) under grant number 416337623.

REFERENCES

1. Vollpracht, A.; Lothenbach, B.; Snellings, R.; Haufe, J. The pore solution of blended cements: a review. *Mater Struct* **2016**, *49*, 3341–3367, doi: 10.1617/s11527-015-0724-1.
2. Vetter, K.J. Dicke und Aufbau von passivierenden Oxydschichten auf Eisen. *Zeitschrift für Elektrochemie* **1957**, 642–648.
3. Andrade, C.; Merino, P.; Nóvoa, X.R.; Pérez, M.C.; Soler, L. Passivation of Reinforcing Steel in Concrete. In *Electrochemical methods in corrosion research V*, Proceedings of the 5th international symposium held in Sesimbra, Portugal, September 5 - 8, 1994. Electrochemical Methods in Corrosion Research V; Ferreira, M.G.S., Ed.; Trans Tech Publ: Aedermannsdorf, 1995; pp 891–898, ISBN 978-0-87849-702-7.
4. Kaesche, H. *Die Korrosion der Metalle*: *Physikalisch-chemische Prinzipien und aktuelle Probleme*, 3., neubearb. und erw. Aufl., Nachdr. 2011 in veränd. Ausstattung; Springer: Heidelberg, 2011, ISBN 978-3-642-18427-7.
5. Glasser, F.P.; Sagoe-Crentsil, K.K. Steel in concrete: Part II Electron microscopy analysis. *Magazine of Concrete Research* **1989**, *41*, 213–220, doi: 10.1680/macr.1989.41.149.213.
6. Ghods, P.; Isgor, O.B.; Brown, J.R.; Bensebaa, F.; Kingston, D. XPS depth profiling study on the passive oxide film of carbon steel in saturated calcium hydroxide solution and the effect of chloride on the film properties. *Applied Surface Science* **2011**, *257*, 4669–4677, doi: 10.1016/j.apsusc.2010.12.120.
7. Freire, L.; Nóvoa, X.R.; Montemor, M.F.; Carmezim, M.J. Study of passive films formed on mild steel in alkaline media by the application of anodic potentials. *Materials Chemistry and Physics* **2009**, *114*, 962–972, doi: 10.1016/j.matchemphys.2008.11.012.
8. Haupt, S.; Strehblow, H.-H. Combined electrochemical and surface analytical investigations of the formation of passive layers. *Corrosion Science* **1989**, *29*, 163–182, doi: 10.1016/0010-938X(89)90027-9.

9. Elsener, B.; Andrade, C.; Gulikers, J.; Polder, R.; Raupach, M. Recommendations of RILEM TC 154-EMC: Electrochemical techniques for measuring metallic corrosion Half-cell potential measurements – Potential mapping on reinforced concrete structures. *Mater Struct* **2003**, *36*, 461–471, doi: 10.1617/13718.
10. Stratfull, R.F. Half-Cell Potentials and the Corrosion of Steel in Concrete. In *Corrosion, concrete and quality control.* 51st Annual Meeting of the Highway Research Board, Washington District of Columbia, United States, 22.-26.01.1973; Highway Research Board National Research Council: Washington, DC, 1973; pp 12–21, ISBN 0309021634.
11. Poursaee, A.; Hansson, C.M. Reinforcing steel passivation in mortar and pore solution. *Cement and Concrete Research* **2007**, *37*, 1127–1133, doi: 10.1016/j.cemconres.2007.04.005.
12. Lothenbach, B.; Winnefeld, F. Thermodynamic modelling of the hydration of Portland cement. *Cement and Concrete Research* **2006**, *36*, 209–226, doi: 10.1016/j.cemconres.2005.03.001.
13. Angst, U.; Elsener, B.; Larsen, C.K.; Vennesland, Ø. Critical chloride content in reinforced concrete – A review. *Cement and Concrete Research* **2009**, *39*, 1122–1138, doi: 10.1016/j.cemconres.2009.08.006.
14. Bertolini, L.; Elsener, B.; Pedeferri, P.; Polder, R. *Corrosion of steel in concrete*: *Prevention, diagnosis, repair*, 1. reprint; Wiley-VCH: Weinheim, 2005, ISBN 3-527-30800-8.
15. Hausmann, D.A. A Probality Model of Steel Corrosion in Conrete. *Materials Selection and Design* **1998**, 64–68.
16. Goñi, S.; Andrade, C. Synthetic concrete pore solution chemistry and rebar corrosion rate in the presence of chlorides. *Cement and Concrete Research* **1990**, *20*, 525–539, doi: 10.1016/0008-8846(90)90097-H.
17. Lambert, P.; PAGE, C.L.; Vassie, P.R.W. Investigations of reinforcement corrosion. 2. Electrochemical monitoring of steel in chloride-contaminated concrete. *Mater Struct* **1991**, *24*, 351–358, doi: 10.1007/BF02472068.
18. Zhang, J. Study on Mechanical Properties of Metakaolin-Based Concretes and Corrosion of Carbon Steel Reinforcement in 3.5% NaCl. *Int. J. Electrochem. Sci. (International Journal of Electrochemical Science)* **2020**, 2883–2893, doi: 10.20964/2020.04.25.
19. Li, C.; Xiao, K. Chloride threshold, modelling of corrosion rate and pore structure of concrete with metakaolin addition. *Construction and Building Materials* **2021**, *305*, 124666, doi:10.1016/j.conbuildmat.2021.124666.
20. Güneyisi, E.; Gesoğlu, M.; Karaboğa, F.; Mermerdaş, K. Corrosion behavior of reinforcing steel embedded in chloride contaminated concretes with and without metakaolin. *Composites Part B: Engineering* **2013**, *45*, 1288–1295, doi: 10.1016/j.compositesb.2012.09.085.
21. Parande, A.K.; Ramesh Babu, B.; Aswin Karthik, M.; Deepak Kumaar, K.K.; Palaniswamy, N. Study on strength and corrosion performance for steel embedded in metakaolin blended concrete/mortar. *Construction and Building Materials* **2008**, *22*, 127–134, doi: 10.1016/j.conbuildmat.2006.10.003.
22. Triana, V.; Lizarazo-Marriaga, J.; Flórez, J.O. Steel corrosion assessment by electrochemical impedance on metakaolin blended mortars. *Mat. Res.* **2013**, *16*, 1457–1464, doi: 10.1590/S1516-14392013005000178.
23. Batis, G.; Pantazopoulou, P.; Tsivilis, S.; Badogiannis, E. The effect of metakaolin on the corrosion behavior of cement mortars. *Cement and Concrete Composites* **2005**, *27*, 125–130, doi: 10.1016/j.cemconcomp.2004.02.041.
24. Ghanem, W.A.; Ghayad, I.M.; Gaber, G.A. Corrosion behavior of reinforcing steel in cement partially replaced with metakaolin in 3.5% NaCl and 5% $MgSO_4$ solution. *International Journal of Metallurgical & Materials Science and Engineering (IJMMSE),* Dec. 2013, 1–8.
25. Homayoonmehr, R.; Ramezanianpour, A.A.; Mirdarsoltany, M. Influence of metakaolin on fresh properties, mechanical properties and corrosion resistance of concrete and its sustainability issues: A review. *Journal of Building Engineering* **2021**, *44*, 103011, doi: 10.1016/j.jobe.2021.103011.
26. Borade, A.N.; Kondraivendhan, B. Corrosion behavior of reinforced concrete blended with metakaolin and slag in chloride environment. *Journal of Sustainable Cement-Based Materials* **2019**, *8*, 367–386, doi: 10.1080/21650373.2019.1566934.
27. PAGE, C.L.; Lambert, P.; Vassie, P.R.W. Investigations of reinforcement corrosion. 1. The pore electrolyte phase in chloride-contaminated concrete. *Mater Struct* **1991**, *24*, 243–252, doi: 10.1007/BF02472078.
28. Kraft, B.; Achenbach, R.; Ludwig, H.-M.; Raupach, M. Hydration and Carbonation of Alternative Binders. *CMD* **2022**, *3*, 19–52, doi: 10.3390/cmd3010003.
29. Deutsches Institut für Normgebung. *Prüfverfahren für Zement*: *Teil 1: Bestimmung der Festigkeit;* Beuth Verlag GmbH: Berlin, 2016, *91.100.10 Zement. Gips. Kalk. Mörte* (DIN EN 196-1).
30. Andrade, C.; Soler, L.; Nóvoa, X.R. Advances in Electrochemical Impedance Measurements in Reinforced Concrete. *MSF* **1995**, *192-194*, 843–856, doi: 10.4028/www.scientific.net/MSF.192-194.843.
31. Orazem, M.E.; Tribollet, B. *Electrochemical impedance spectroscopy;* Wiley: Hoboken, NJ, 2008, ISBN 978-0-470-04140-6.
32. Ghods, P.; Isgor, O.B.; McRae, G.; Miller, T. The effect of concrete pore solution composition on the quality of passive oxide films on black steel reinforcement. *Cement and Concrete Composites* **2009**, *31*, 2–11, doi: 10.1016/j.cemconcomp.2008.10.003.
33. Feliu, V.; González, J.A.; Adrade, C.; Feliu, S. Equivalent circuit for modelling the steel-concrete interface. II. Complications in applying the stern-geary equation to corrosion rate determinations. *Corrosion Science* **1998**, *40*, 995–1006, doi: 10.1016/S0010-938X(98)00037-7.
34. Sánchez, M.; Gregori, J.; Alonso, C.; García-Jareño, J.J.; Takenouti, H.; Vicente, F. Electrochemical impedance spectroscopy for studying passive layers on steel rebars immersed in alkaline solutions simulating concrete pores. *Electrochimica Acta* **2007**, *52*, 7634–7641, doi: 10.1016/j.electacta.2007.02.012.
35. Cai, Y.; Zheng, H.; Hu, X.; Lu, J.; Poon, C.S.; Li, W. Comparative studies on passivation and corrosion behaviors of two types of steel bars in simulated concrete pore solution. *Construction and Building Materials* **2021**, *266*, 120971, doi: 10.1016/j.conbuildmat.2020.120971.
36. Flis, J.; Zakroczymski, T. Impedance Study of Reinforcing Steel in Simulated Pore Solution with Tannin. *J. Electrochem. Soc.* **1996**, *143*, 2458, doi: 10.1149/1.1837031.

37. Volpi, E.; Olietti, A.; Stefanoni, M.; Trasatti, S.P. Electrochemical characterization of mild steel in alkaline solutions simulating concrete environment. *Journal of Electroanalytical Chemistry* **2015**, *736*, 38–46, doi: 10.1016/j.jelechem.2014.10.023.
38. Andrade, C. Propagation of reinforcement corrosion: principles, testing and modelling. *Mater Struct* **2019**, *52*, 1–26, doi: 10.1617/s11527-018-1301-1.
39. Barsoukov, E.; Macdonald, J.R. Impedance Spectroscopy: Theory, Experiment, and Applications.
40. Urquidi-Macdonald, M.; Real, S.; Macdonald, D.D. Application of Kramers-Kronig Transforms in the Analysis of Electrochemical Impedance Data: II . Transformations in the Complex Plane. *J. Electrochem. Soc.* **1986**, *133*, 2018–2024, doi: 10.1149/1.2108332.
41. Duffó, G.S.; Farina, S.B. Electrochemical behaviour of steel in mortar and in simulated pore solutions: Analogies and differences. *Cement and Concrete Research* **2016**, *88*, 211–216, doi: 10.1016/j.cemconres.2016.07.007.